Hindawi Publishing Corporation
Advances in Materials Science and Engineering
Volume 2015, Article ID 148657, 6 pages
http://dx.doi.org/10.1155/2015/148657

Research Article

Microstructure and Mechanical Property of Hot-Pressed Al_2O_3-Ni-P Composites Using Ni-P-Coated Al_2O_3 Powders

Hyeong-Chul Kim[1] and Jae-Kil Han[2]

[1]*Department of Mechanical Engineering, University of Incheon, 12-1 Songdo-dong, Yeonsu-gu, Incheon 406-772, Republic of Korea*
[2]*Technology Convergence Center, Incheon Techno Park, Gaetbeol-ro 12, Songdo-dong, Yeonsu-gu, Incheon 406-840, Republic of Korea*

Correspondence should be addressed to Jae-Kil Han; jkhan@itp.or.kr

Received 18 September 2015; Revised 11 December 2015; Accepted 14 December 2015

Academic Editor: Wenbin Yi

Al_2O_3-Ni-P composite powders with Ni-P contents of 10.9, 14.4, and 20.4 wt.% were synthesized via the Ni-P electroless deposition process. The as-received Al_2O_3-Ni-P composite powders were composed of Ni-P particles and Ni-P coating layer. Some Ni-P particles randomly adhered to the Al_2O_3 powders, and their particle diameter ranged from 5 nm to 20 nm. The thin Ni-P layer had about 5 nm thick amorphous structure and directly bonded with Al_2O_3 powders. Using the Ni-P-coated Al_2O_3 powders, a dense Al_2O_3-Ni-P composite can be successfully obtained using the hot press process at 1,350°C for 1 hour in an Ar atmosphere under an applied pressure of 30 MPa. The hot-pressed Al_2O_3-15 wt.% Ni-P composite showed excellent material properties. Its relative density, Vickers hardness, and fracture toughness were comparatively high: about 99.1%, 2,360 Hv, and 6 MPa·$m^{1/2}$, respectively. The fracture surface of the hot-pressed Al_2O_3-Ni-P composite showed a semiductile mode due to the mixed intergranular and transgranular fracture mode. In particular, the fracture toughness of the hot-pressed Al_2O_3-15 wt.% Ni-P composite was strongly enhanced by the combined action of the crack branching and the crack deflection.

1. Introduction

Aluminum oxide has been used in structural components in the last 100 years [1]. Due to its intrinsic properties such as its high chemical stability, corrosion stability, wear resistance, and elastic modulus, it has also been recently used in bioceramics as a dental material and in various body and bone replacement parts and augmentation parts [2–4]. However, its use was limited because of its inherent brittleness and poor impact strength. Therefore, the improvement of its mechanical properties has been considered a toughening mechanism though the microstructures control approach. The microstructural improvement of aluminum oxide, such as its fine particle and grain size, is expected to enhance its fracture strength according to the Hall-Petch equation [5]. Furthermore, a toughening mechanism using a second phase addition of metallic materials such as Ni, Co, Mo, and Ag can efficiently reduce the crack propagation because the dispersion of the ductile metals caused the plastic deformation [6, 7]. There were many reports on the fabrication of metal-ceramic composites using a conventional method such as ball milling [8], attrition milling [9], sol-gel [10], and electroless deposition [11–13]. Among them, electroless deposition is regarded as a good method of synthesizing a homogeneous metal-ceramic composite. This method allows easy control of coating thickness, even dispersion of the metal coating, and homogeneous distribution of all the components.

An electroless deposited Ni-P composite has a great potential for industrial applications due to its high degree of hardness, excellent corrosion, and wear resistance [14, 15]. An amorphous Ni-P composite is transformed to the nanocrystalline state during heat treatments, after which its mechanical properties are further improved [16].

In this study, homogeneous Ni-P-coated Al_2O_3 powders were prepared via electroless deposition. Al_2O_3-Ni-P sintered bodies were obtained via hot pressing which simultaneously applied heat and pressure. Hot pressing has several benefits such as the achievement of a high density, the minimization

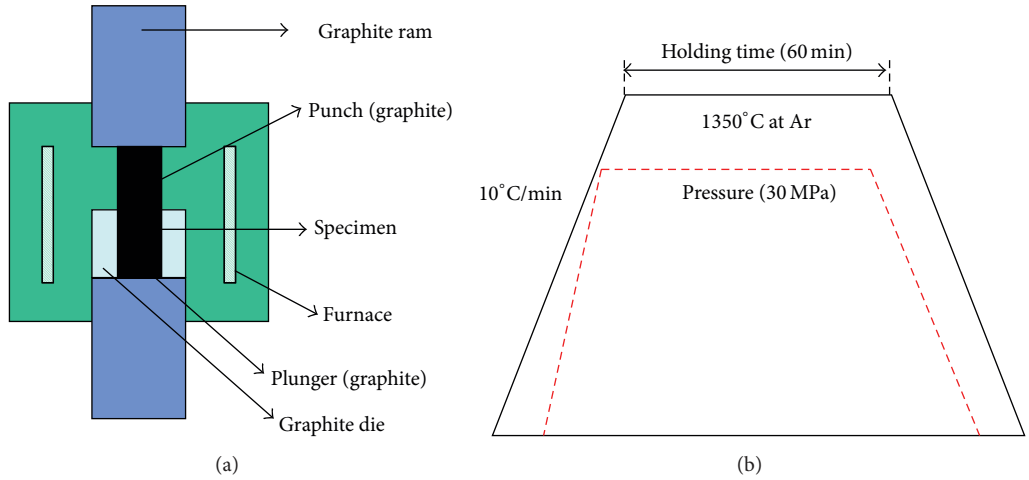

Figure 1: A schematic diagram (a) and sintering conditions (b) of the hot pressing.

of the grain growth and the heterogeneous grain growth, and the high accuracy of shaping the production [17]. To understand the formation of hot-pressed sintered bodies from Al_2O_3 powders prepared via Ni-P electroless deposition, the microstructure and the crystal structure were investigated using the Ni-P-coated Al_2O_3 powders, which were produced at different concentrations. The material properties and fracture mode of the hot-pressed Al_2O_3-Ni-P composites were also investigated.

2. Experimental Procedure

Ni-P-coated Al_2O_3 powders were synthesized via Ni-P electroless deposition. Electroless Ni-P deposits were produced using nickel sulfate hexahydrate ($NiSO_4{\cdot}6H_2O$) as the nickel source, sodium phosphinate monohydrate ($NaH_2PO_2{\cdot}H_2O$) as the reducing agent, sodium acetate trihydrate ($CH_3COONa{\cdot}3H_2O$) as the complexing agent, and sodium dodecyl sulfate as the stabilizer. The composition of the Ni-P plating solutions used was as follows: 9 g/L of $NaH_2PO_2{\cdot}H_2O$, 5 g/L of $CH_3COONa{\cdot}3H_2O$, and 0.005 g of sodium dodecyl sulfate. And then the concentration of $NiSO_4{\cdot}6H_2O$ was varied from 15 g/L, 25 g/L to 35 g/L. Afterward, 30 g of α-Al_2O_3 powders (Sumitomo Chem. Co.) with an average diameter of 200 nm added to the Ni-P plating solution. The temperature of the coating bath was kept at 85°C, and the pH of the bath was kept at 5.0 through the addition of acetic acid. The Ni-P electroless deposition time on α-Al_2O_3 powders was increased by 2, 4, and 6 hours. According to the reaction time, the Ni concentrations of the synthesized Ni-P deposits measured via ICP-AES were about 10.9%, 14.4%, and 20.4%, respectively. To eliminate the residual organic component of the coating process, the Ni-P-coated Al_2O_3 powders were washed using a diluted hydrochloric acid solution and deionized water. To neutralize the acidic solution, the Ni-P-coated Al_2O_3 powders were washed repeatedly using ammonia water and rinsed with deionized water. Then the Al_2O_3-Ni-P powders were centrifugally separated and dried at 80°C for 6 hours.

The sintering was carried out using the hot press. The as-received Al_2O_3-Ni-P powders were sintered at 1,350°C for 1 hour in an Ar atmosphere under an applied pressure of 30 MPa. The pressure and temperature were raised simultaneously, and the applied pressure after 1,200°C was achieved at 30 MPa, which was maintained for 1 h. The diagram and experimental conditions of the hot press are shown in Figure 1. Each side of the hot-pressed samples was polished to remove the surfaces in contact with the graphite mold and the BN powders. The crystal structures of the Al_2O_3-Ni-P powders and the hot-pressed composite were identified via X-ray diffraction (D/MAX250, Rigaku, Japan) with CuKα radiation (λ = 1.54056 Å). FE-SEM (JSM 6335F, JEOL, Japan) and TEM (JEM 2010, JEOL, Japan) were used to observe crack propagations and fracture surfaces. The relative densities of hot-pressed samples were measured using Archimedes' method. Vickers hardness was measured by indenting with 500 g load. The fracture toughness was calculated via the indentation method [18] using 20 kg load.

3. Results and Discussion

Figure 2 shows the TEM (a) and HRTEM (b) images of the raw α-Al_2O_3 powders. The raw α-Al_2O_3 particles showed a spherical shape with a diameter of about 200 and were agglomerated each other due to the mutual attraction among the particles. In the HRTEM image in Figure 2(b), the two-dimensional lattice images clearly appeared in the inner region and the surface regions of the raw α-Al_2O_3 powders.

Figure 3 shows the TEM (a) and HRTEM (b) images of the Al_2O_3-10 wt.% Ni-P powders synthesized via Ni-P electroless deposition. Ni-P particles with 5 nm to 20 nm diameters were attached to the α-Al_2O_3 powders and randomly dispersed around the α-Al_2O_3 powders. In Figure 3(b), which shows the cross-sectional image of the Al_2O_3-10 wt.% Ni-P powders, the α-Al_2O_3 powders were homogeneously coated with about 5 nm amorphous Ni-P coating, that is, with a core-sell structure. Ni-P coating layer directly bonded with the α-Al_2O_3 powders without defects at the interface.

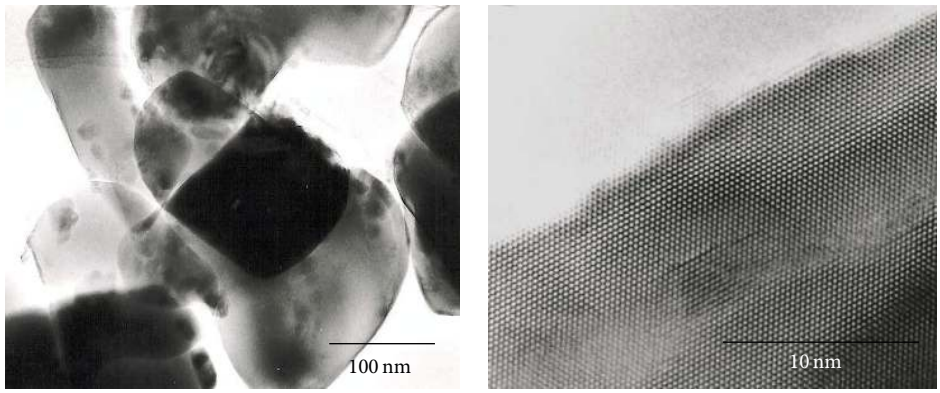

(a) (b)

Figure 2: TEM (a) and HRTEM (b) of images of the raw α-Al_2O_3 powders.

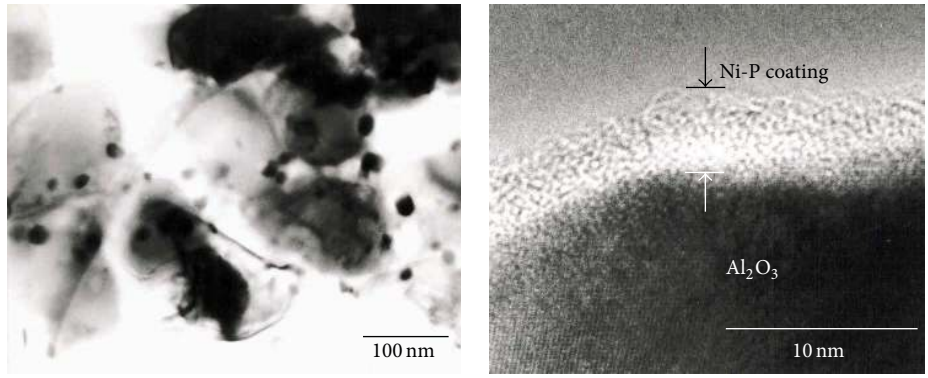

(a) (b)

Figure 3: TEM (a) and HRTEM (b) of images of the Al_2O_3-10 wt.% Ni-P powders synthesized by Ni-P electroless deposition process.

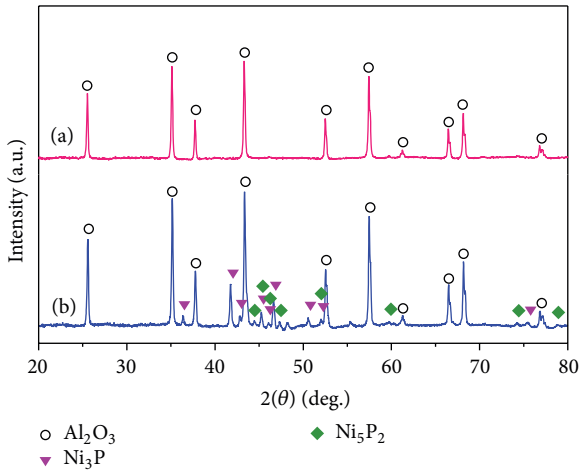

Figure 4: XRD profiles of the (a) as-received Al_2O_3-10 wt.% Ni-P powders and (b) Al_2O_3-10 wt.% Ni-P powders calcined at 450°C after electroless Ni-P coating process.

Figure 4 shows the XRD profiles of (a) the as-received Al_2O_3-10 wt.% Ni-P powders and (b) the Al_2O_3-10 wt.% Ni-P powders calcined at 450°C after the electroless Ni-P coating. The as-received Al_2O_3-10 wt.% Ni-P powders were not detected at the Ni-P and Ni peaks after the Ni-P electroless deposition. After such powders were calcined at 450°C, the strong intensity of Ni_3P peaks was detected and a small amount of Ni_5P_2 peaks was also detected. These results indicate that initial state of the coating layer existed in an amorphous Ni-P phase due to the nondetection of the Ni peaks and that after the burn out the amorphous Ni-P phase was crystallized to intermediate phases such as Ni_5P_2 and Ni_3P.

To clearly understand the microstructure of the hot-pressed Al_2O_3-Ni-P composites, TEM observation was carried out. Figure 5 shows the TEM micrographs of the hot-pressed Al_2O_3-10 wt.% Ni-P composite. In Figure 5(a), the white and dark regions correspond with the α-Al_2O_3 and Ni-P grains, respectively. Ni-P particles with a wide particle size distribution of 100–800 nm were dispersed homogeneously in α-Al_2O_3 and were located at the grain boundary and triple junction. The grain size of α-Al_2O_3 was evaluated to be about 300 nm to 1.2 μm and a small amount of pores was observed. Figure 5(b), the enlarged TEM image, shows that microcracks were not found on the interface and the Ni-P particles directly bonded with α-Al_2O_3 matrix.

Table 1: Ni contents and material properties of Al_2O_3 and hot-pressed Al_2O_3-Ni-P composites.

	Ni content (wt.%)	Hardness (kgf/mm^2)	Relative density (g/L)	Fracture toughness (MPa·m$^{1/2}$)
Al_2O_3	—	1834	96.2%	2.6
Al_2O_3-10 wt.% Ni_3P	10.9	2130	98.0%	5.1
Al_2O_3-15 wt.% Ni_3P	14.4	2358	99.1%	5.9
Al_2O_3-20 wt.% Ni_3P	20.4	2185	98.5%	4.7

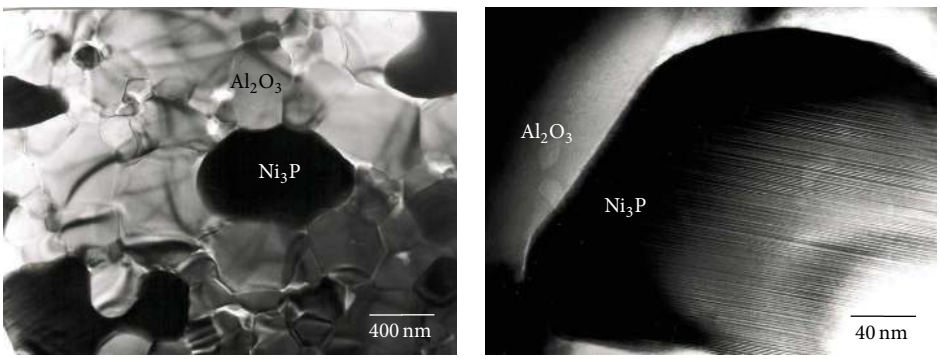

(a) (b)

Figure 5: TEM (a) and HRTEM (b) images of hot-pressed Al_2O_3-Ni-P composite.

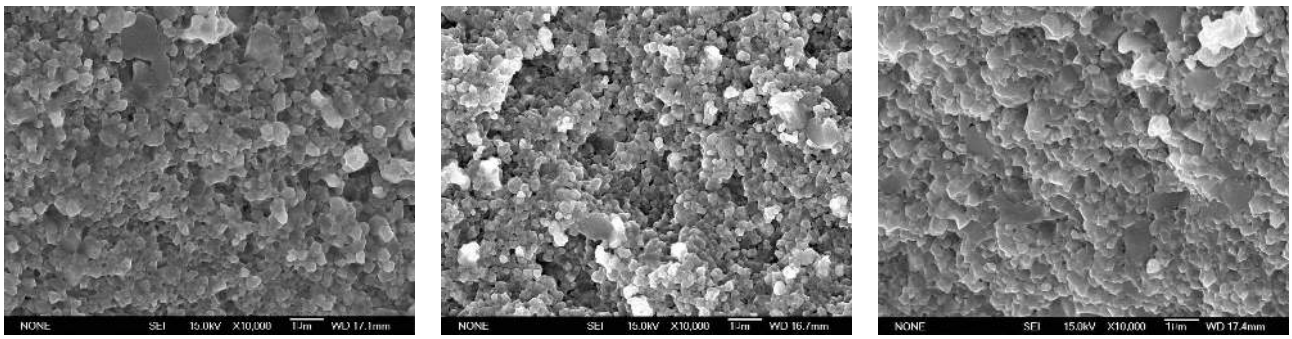

(a) (b) (c)

Figure 6: SEM images of the fracture surface of hot-pressed (a) Al_2O_3-10 wt.% Ni-P, (b) Al_2O_3-15 wt.% Ni-P, and (c) Al_2O_3-20 wt.% Ni-P composites.

Ni contents and material properties of the hot-pressed Al_2O_3-Ni-P composites are summarized in Table 1. The relative densities of the hot-pressed Al_2O_3-Ni-P composites were over 98.0% and Al_2O_3-15 wt.% Ni-P composite showed a high value of about 99.1%. In the samples hot-pressed at 1,350°C for 1 h under 30 MPa, Vickers hardness remarkably increased to about 2,360 Hv, perhaps due to the high densification and minimization of the grain growth. The fracture toughness of the hot-pressed Al_2O_3-Ni-P composites showed enhanced values of about 4.7–5.9 MPa·m$^{1/2}$, about 2.0 times higher than the value of α-Al_2O_3 prepared under pressureless sintering. In general, the dispersion of the ductile phase in the ceramic matrix grains can efficiently reduce the crack propagation and also tends to switch to the transgranular fracture mode [19–21].

Figure 6 shows the SEM micrographs of the fracture surfaces of the hot-pressed Al_2O_3-Ni-P composites. The fracture surfaces show the semiductile mode due to mixed intergranular and transgranular fracture mode. In the case of the hot-pressed Al_2O_3-15 wt.% Ni-P composite with the highest fracture toughness, the main fracture mode was the intergranular type, which showed the crack deflection and toughening mechanism.

Figure 7 shows the SEM images of the crack propagation from the hot-pressed Al_2O_3-15 wt.% Ni-P composite. The crack branching and crack deflection were observed in the hot-pressed Al_2O_3-Ni-P composites. In Figure 7(b), an enlarged SEM image, crack branching, and crack deflection were evidently found, and very fine spherical Ni-P particles were homogeneously embedded on the surface. The fracture

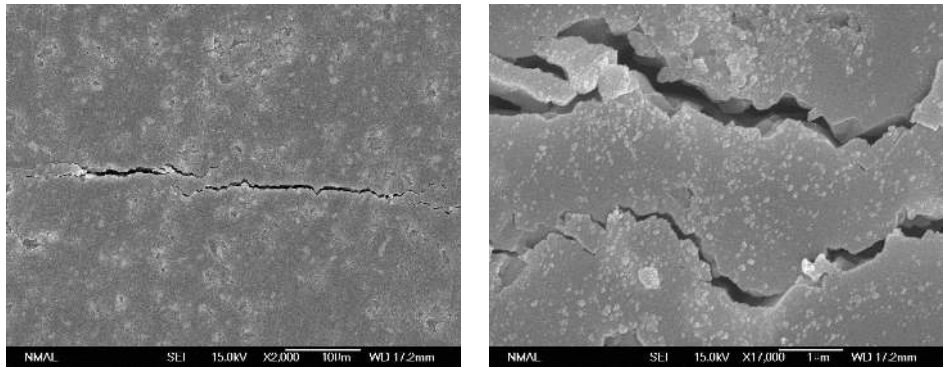

(a) (b)

Figure 7: SEM image (a) and enlarged SEM image (b) of crack propagation from hot-pressed Al_2O_3-15 wt.% Ni-P composite.

toughness of the hot-pressed Al_2O_3-15 wt.% Ni-P composite was strongly enhanced due to the combined action of the crack branching and the crack deflection.

4. Conclusion

From the study on the microstructure of Al_2O_3-Ni-P composite powders synthesized via electroless deposition and from the characterization of their hot-pressed Al_2O_3-Ni-P composite, the following results were obtained:

(1) In the as-received Al_2O_3-Ni-P composite powders, Ni-P contents of the Ni-P-coated Al_2O_3 powders were measured as 10.9, 14.4, and 20.4 wt.%. Al_2O_3 surface was directly coated with the nanosized Ni-P coating layer with an amorphous structure, and the coating layer was about 5 nm thick. Also, the nanosized Ni-P particles with particle sizes of 5–20 nm randomly adhered to Al_2O_3 powders and existed between Al_2O_3 powders.

(2) In Al_2O_3-Ni-P composite powders calcined at 450°C, the coating layer of the amorphous Ni-P phase was crystallized to the intermediate phases, which consisted of a large amount of Ni_3P and a small amount of Ni_5P_2 phase.

(3) The hot-pressed Al_2O_3-15 wt.% Ni-P composite showed excellent material properties such as a high relative density, Vickers hardness, and fracture toughness of about 99.1%, 2,360 Hv, and 6 MPa·$m^{1/2}$, respectively.

(4) The fracture toughness of Al_2O_3-Ni-P composite was increased by two times of that of α-Al_2O_3 pressureless sintered body due to the plastic deformation mechanism of the ductile phase like Ni-P. The main fracture mode showed the intergranular type ductile fracture mode. The microindentation results showed that the toughening mechanism of the combined crack branching and crack deflection decreased the crack propagation.

Conflict of Interests

The authors declare that there is no conflict of interests regarding the publication of this paper.

Acknowledgment

This study was supported by a University of Incheon Research Grant in 2012.

References

[1] J. Ahn and J. W. Rabalais, "Composition and structure of the $Al_2O_3$0001-(1×1) surface," *Surface Science*, vol. 388, no. 1-3, pp. 121–131, 1997.

[2] S. M. Kurtz, S. Kocagöz, C. Arnholt, R. Huet, M. Ueno, and W. L. Walter, "Advances in zirconia toughened alumina biomaterials for total joint replacement," *Journal of the Mechanical Behavior of Biomedical Materials*, vol. 31, pp. 107–116, 2014.

[3] E. Soh, E. Kolos, and A. J. Ruys, "Foamed high porosity alumina for use as a bone tissue scaffold," *Ceramics International*, vol. 41, no. 1, pp. 1031–1047, 2015.

[4] A. H. De Aza, J. Chevalier, G. Fantozzi, M. Schehl, and R. Torrecillas, "Crack growth resistance of alumina, zirconia and zirconia toughened alumina ceramics for joint prostheses," *Biomaterials*, vol. 23, no. 3, pp. 937–945, 2002.

[5] Y. S. Sato, M. Urata, H. Kokawa, and K. J. Ikeda, "Hall-petch relationship in friction stir welds of equal channel angular-pressed aluminium alloys," *Materials Science and Engineering A*, vol. 354, no. 1-2, pp. 298–305, 2003.

[6] Z. Pang, A. Chughtai, I. Sailer, and Y. Zhang, "A fractographic study of clinically retrieved zirconia–ceramic and metal-ceramic fixed dental prostheses," *Dental Materials*, vol. 31, no. 10, pp. 1198–1206, 2015.

[7] V. M. Sglavo, F. Marino, B. R. Zhang, and S. Gialanella, "Ni_3Al intermetallic compound as second phase in Al_2O_3 ceramic composites," *Materials Science and Engineering A*, vol. 239-240, pp. 665–671, 1997.

[8] J. Li, F. Li, and K. Hu, "Preparation of Ni/Al_2O_3 nanocomposite powder by high-energy ball milling and subsequent heat treatment," *Journal of Materials Processing Technology*, vol. 147, no. 2, pp. 236–240, 2004.

[9] C. Zhang, R. Janssen, and N. Claussen, "Pressureless sintering of β-sialon with improved green strength by using metallic Al powder," *Materials Letters*, vol. 57, no. 22-23, pp. 3352–3356, 2003.

[10] Y. L. Huang, D. S. Xue, P. H. Zhou, Y. Ma, and F. S. Li, "α-Fe–Al_2O_3 nanocomposites prepared by sol-gel method," *Materials Science and Engineering A*, vol. 359, no. 1-2, pp. 332–337, 2003.

[11] J. Michalski, K. Konopka, and M. Trzaska, "Description of Al_2O_3 powders coated by Ni-P particles obtained through an electroless chemical reaction and possibilities to obtain an Al_2O_3/Ni-P composite," *Materials Chemistry and Physics*, vol. 81, no. 2-3, pp. 407–410, 2003.

[12] J. F. Silvain, J. L. Bobet, and J. M. Heintz, "Electroless deposition of copper onto alumina sub-micronic powders and sintering," *Composites Part A: Applied Science and Manufacturing*, vol. 33, no. 10, pp. 1387–1390, 2002.

[13] E. Natividad, E. Lataste, M. Lahaye, J. M. Heintz, and J. F. Silvain, "Chemical and morphological study of the sensitisation, activation and Cu electroless plating of Al_2O_3 polycrystalline substrate," *Surface Science*, vol. 557, no. 1–3, pp. 129–143, 2004.

[14] S. M. Monir Vaghefi, A. Saatchi, and M. Ebrahimian-Hoseinabadi, "Deposition and properties of electroless Ni-P-B_4C composite coatings," *Surface and Coatings Technology*, vol. 168, no. 2-3, pp. 259–262, 2003.

[15] V. V. N. Reddy, B. Ramamoorthy, and P. K. Nair, "A study on the wear resistance of electroless Ni–P/diamond composite coatings," *Wear*, vol. 239, no. 1, pp. 111–116, 2000.

[16] I. Apachitei, J. Duszczyk, L. Katgerman, and P. J. B. Overkamp, "Electroless Ni-P composite coatings: the effect of heat treatment on the microhardness of substrate and coating," *Scripta Materialia*, vol. 38, no. 9, pp. 1347–1353, 1998.

[17] S. A. Baldacim, C. A. A. Cairo, and C. R. M. Silva, "Mechanical properties of ceramic composites," *Journal of Materials Processing Technology*, vol. 119, no. 1–3, pp. 273–276, 2001.

[18] S. A. Baldacim, C. Santos, K. Strecker, O. M. M. Silva, and C. R. M. Silva, "Development and characterization by HRTEM of hot-pressed Si_3N_4–SiC(w) composites," *Journal of Materials Processing Technology*, vol. 169, no. 3, pp. 445–451, 2005.

[19] J. Lu and J. A. Szpunar, "Microstructural model of intergranular fracture during tensile tests," *Journal of Materials Processing Technology*, vol. 60, no. 1–4, pp. 305–310, 1996.

[20] M. Szutkowska, "Fracture resistance behavior of alumina-zirconia composites," *Journal of Materials Processing Technology*, vol. 153-154, no. 1–3, pp. 868–874, 2004.

[21] F. Z. Yang, J. Zhao, and X. Ai, "Effect of initial particulate and sintering temperature on mechanical properties and microstructure of WC-ZrO_2-VC ceramic composites," *Journal of Materials Processing Technology*, vol. 209, no. 9, pp. 4531–4536, 2009.